COBEM 2023 27TH INTERNATIONAL CONGRESS OF MECHANICAL ENGINEERING

ABCM Brazilian Society of Mechanical Sciences and Engineering
27th ABCM International Congress of Mechanical Engineering
December 04-08, 2023, Florianópolis-SC, Brazil

COB-2023-0349
THE PERFORMANCE OF A SUCTION VALVE INSTALLED ON THE PISTON OF A VARIABLE-SPEED RECIPROCARING COMPRESSOR

Willian T. F. D. Silva
Cesar J. Deschamps
POLO Research Laboratories for Emerging Technologies in Cooling and Thermophysics
Federal University of Santa Catarina
Florianópolis – Brazil
willian.duarte@polo.ufsc.br; deschamps@polo.ufsc.br

Abstract. The suction valve is usually installed on the cylinder head of small reciprocating compressors. However, due to the current trend of miniaturizing compressors, an alternative is to install the suction valve on the piston head in order to increase the valve passage area. This article reports an investigation concerning the performance of the suction placed on the cylinder head and piston for different compressor speeds. A validated numerical model was used to simulate the compressor for both configurations under different operating conditions. The results showed that the suction valve dynamics is very sensitive to changes in the compressor speed and can significantly affect the compressor performance. Furthermore, we found that valves with the same passage area and dynamic characteristics perform worse when installed on the piston head in comparison with the valve on the cylinder head. Despite significantly reducing the compressor volumetric efficiency, the suction gas superheating associated with the valve on the piston was not influenced by the compressor speed. The findings of this study provide valuable information for the design and optimization of variable-speed compressors as far as efficiency and reliability are concerned.

Keywords: *reciprocating compressor; suction valve; efficiency breakdown; variable-speed*

1. INTRODUCTION

The miniaturization of compressors has been a trend in recent years, as the demand for compact, efficient, and portable devices has increased. The miniaturization of reciprocating compressors gives rise to the size reduction of cylinder heads, as manufacturers strive to develop compact, efficient devices that meet the needs of their customers. However, there are some design challenges associated with the suction orifice area, since it regulates the mass flow rate of refrigerant into the compression chamber, directly affecting the compressor efficiency. In fact, as the size of the cylinder head is decreased, the size of the suction orifice must also be reduced, decreasing the effective area available for suction process and hence increasing the head loss that reduce the compressor volumetric and isentropic efficiencies.

Considering these challenges, innovative solutions must be developed to make the miniaturization of reciprocating compressors feasible. An alternative put forward in recent years is to place the suction valve directly on the piston head. Wu et al. (2022) pointed out that the stiffness of the valve on the piston should be greater than that on the cylinder head to avoid high lift, and consequently, high valve impact speeds. Also, due to the high temperature of the piston wall, suction gas superheating losses can increase greatly, decreasing the volumetric efficiency.

This article presents a numerical analysis regarding the performance of a reciprocating compressor with the suction valve on the piston head. The model developed by Silva et al. (2022) has been used to simulate a small household reciprocating compressor (swept volume of 6.52 cm³) operating with R600a under a speed range from 1800 to 6300 rpm.

2. METHODOLOGY

2.1 Suction valve on the piston

The operation of the suction valve on the piston can be described with the assistance of Figure 1. As the piston passes the top dead center, it accelerates downward with increasing absolute velocity (I). This motion continues through the re-expansion process until the pressure in the compression chamber reaches the pressure in the suction chamber, when the suction valve opens. The motion of the piston gives rise to inertial force that assists the valve opening (II). As the suction process proceeds with the valve open, eventually the piston reached its maximum velocity. The deceleration that follows implies that the inertial force act to move the suction valve towards the piston (III). After reaching the bottom dead center, the piston begins its upward movement and the increase of pressure in the compression chamber act to close the valve (IV).

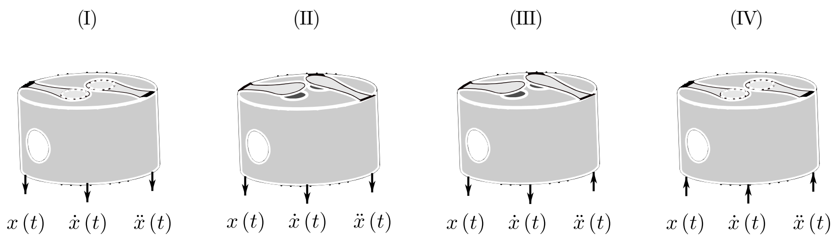

Figure 1 - Suction valve on the piston.

2.2 Simulation model

The compressor simulation model depicted in Figure 2 was implemented using the commercial software GT-SUITE, being formed by volumes connected to pipes (SILVA et al., 2022). The instantaneous piston position is obtained as follows:

$$x(t) = d_{TDC} - \{e_c \cos\theta + [L_r^2 - (e_c \sin\theta - d_m)^2]^{1/2}\}, \tag{1}$$

where d_{TDC}, e_c, L_r and d_m are the distance between TDC and BDC, the eccentric ratio of the compressor mechanism, the length of the connection rod, and the cylinder offset, respectively. With the instantaneous piston position, the instantaneous volume of the compression chamber can be obtained by multiplying Eq. (1) by the piston area.

The instantaneous temperature inside the compression chamber is calculated via the first law of thermodynamics, with the wall heat transfer estimated with the correlation proposed by Disconzi et al. (2012). With estimates of temperature and specific mass determined from the mass conservation equation in the compression chamber, the pressure inside the compression chamber can be obtained from the Refprop database (LEMMON, 2018).

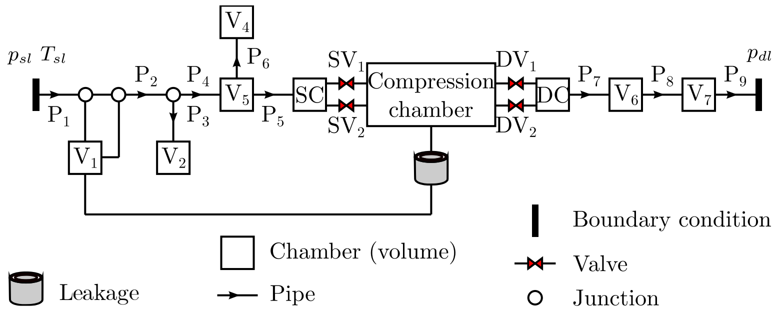

Figure 2 - Schematic gas flow structure of the entire simulation compressor model.

Valve dynamics is modeled as a single-degree-of-freedom spring-damper-mass system. The fluid flow in the suction and discharge mufflers is numerically solved with a one-dimensional CFD approach (DESCHAMPS et al., 2002), based on the finite-volume method and an explicit time scheme. Mass flow rate through valves is calculated using the concept of effective flow area with reference to one-dimensional isentropic flow in a convergent nozzle, taking into account viscous friction effects (LINK and DESCHAMPS, 2010).

The time-step was restricted to the Courant-Friedrichs-Lewy criterion smaller than 0.7 to ensure the numerical stability of the solution procedure. The boundary conditions adopted in the simulation model were the evaporating and condensing pressures, the temperature at the compressor inlet and the temperature of the external environment. The solution procedure converged when differences of less than 0.2% were found for pressure and mass flow rate and less than 0.1 K for temperatures between two consecutive compression cycles.

2.3 Thermal model

The thermal model used in the simulations is essentially that used by Silva et al. (2022), following a hybrid approach in which the compressor is divided into several non-overlapping control volumes. The general equation applied to each control volume has the form of Eq. (1). The compressor components and the non-linear system of equations of the compressor thermal sub-model are presented in Tab 1.

$$\sum \dot{Q} + \sum_{i}^{N} UA_{ij}(T_j - T_i) = 0, \tag{2}$$

For the valve on the piston configuration, the thermal model requires some modifications. Despite the assumption that the suction muffler remains essentially the same regardless of the valve configuration, a different approach must be used for the temperature of the suction muffler wall. In this respect, no control volume is adopted for the suction muffler when the valve is installed on the piston. Consequently, the temperature of the suction muffler wall is assumed to be equal to the cylinder temperature. Therefore, the control volumes for the compression chamber and the suction muffler are combined into a single control volume, as depicted in Figure 3.

Table 1 - Energy balances of the compressor thermal network.

Control volume	$\sum \dot{Q}$	$\sum_{i}^{N} UA_{ij}(T_j - T_i)$
Suction muffler	$\dot{Q}_{sm,w}$	$UA_{ie-sm}(T_{ie} - T_{sm,w})$
Compression chamber	$\dot{Q}_{cyl,w} + \dot{Q}_{pc}$	$UA_{ie-wall}(T_{ie} - T_{cyl,w})$
Valve plate	$\dot{Q}_{plate}$	$UA_{dc-plate}(T_{dc} - T_{cyl,plate})$
Discharge chamber	$\dot{Q}_{dc}$	$UA_{dc-plate}(T_{dc} - T_{cyl,plate})$
Discharge muffler	$\dot{Q}_{dm,w}$	$UA_{ie-dm}(T_{ie} - T_{dm,w})$
Discharge tube	$\dot{Q}_{dt,w}$	$UA_{ie-dt}(T_{ie} - T_{dt,w})$
Oil	$\dot{Q}_b$	$UA_{sh-oil}(T_{sh} - T_{oil})$
Motor	$\dot{Q}_m$	$UA_{ie-mot}(T_{ie} - T_m)$
Internal environment	$(1-\varphi)\dot{m}_{sl}(h_{sl} - h_{ie}) + \dot{m}_l(h_l - h_{ie})$	$UA_{ie-sm}(T_{sm,w} - T_{ie}) + UA_{ie-wall}(T_{cil,w} - T_{ie}) + UA_{ie-dm}(T_{dm,w} - T_{ie}) + UA_{dt-ie}(T_{dt,w} - T_{ie}) + UA_{ie-mot}(T_{mot} - T_{ie}) + UA_{ie-sh}(T_{sh} - T_{ie})$
Shell	-	$UA_{sh-oil}(T_{oil} - T_{sh}) + UA_{ie-sh}(T_{ie} - T_{sh}) + UA_{sh-amb}(T_{amb} - T_{sh})$

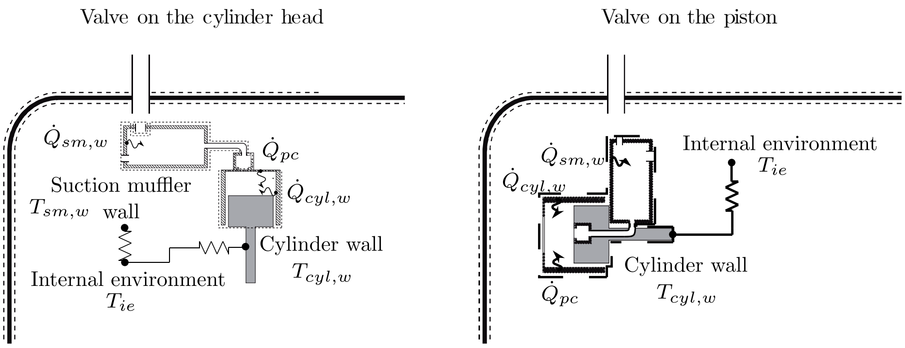

Figure 3 - Comparison between thermal model for valve on the cylinder head (left) and valve on the piston (right).

2.4 Valve dynamics

Figure 4 shows a schematic of the single-degree-of-freedom spring-damper-mass system used to simulate a suction valve on the piston, subjected to a harmonic motion of the piston. By applying D'Alembert's principle, it follows that:

$$M_v\ddot{y} + C_v\dot{y} + K_v y = C_v\dot{x} + K_v x + F_{\Delta p} + F_{st}, \tag{3}$$

where M_v, C_v and K_v represent the equivalent mass, damping coefficient and stiffness of the reed valve, respectively. Moreover, F_{st} is the valve stiction force due to the presence of lubricant oil, estimated by the model of Pizarro-Recabarren et al. (2013), and $F_{\Delta p}$ is the force due to the pressure load on the reed, calculated using the concept of effective force area

(PEREIRA and DESCHAMPS, 2011). As the piston position x(t) is known from Eq. (1), equation of the valve dynamics can also be expressed as:

$$M_v \ddot{y} + C_v \dot{y} + K_v y = F_{pis} + F_{\Delta p} + F_{st}, \tag{4}$$

where:

$$F_{pis} = K_v \left[d_{TDC} - \sqrt{L_r^2 - (e_c \sin\theta - d_m)^2} - e_c \cos\theta \right] + C_v \dot{\theta} \left[\frac{e_c \cos\theta\,(e_c \sin\theta - d_m)}{\sqrt{c^2 - (e_c \sin\theta - d_m)^2}} + e_c \sin\theta \right], \tag{5}$$

As a result, the valve excitation is equivalent to applying a harmonic force of magnitude F_{pis} to a mass in a fixed reference system. This force is related to the crank angle angular speed, $\dot{\theta}$, which varies with the compressor rotational speed. Hence, the magnitude of the harmonic force is expected to increase with the compressor speed, and the same with the inertial effect on the suction valve associated with the piston motion. Naturally, for the valve configuration installed in the cylinder head, there is no such an excitation and, therefore, $F_{pis} = 0$.

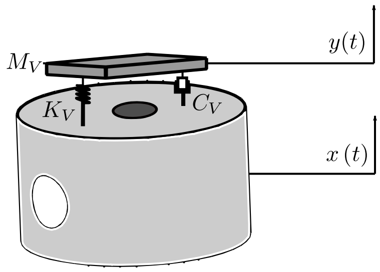

Figure 4 - 1d spring-damper-mass system of the valve on the piston.

3. COMPRESSOR THERMODYNAMIC PERFORMANCE

The thermodynamic performance of hermetic reciprocating compressors is characterized by the volumetric efficiency and exergetic efficiency. A procedure has been recently proposed to detach these efficiencies into their main components (physical sub-processes) to identify the main sources of inefficiencies. As the focus of this paper is the suction valve, the detachment presented herein is concerned with the inefficiencies associated with the suction process.

3.1 Volumetric efficiency

The volumetric efficiency is defined as the ratio between the actual mass flow rate ($\dot{m}$) and the theoretical mass flow rate ($\dot{m}_{th}$). The theoretical mass flow rate is attributed to an idealized compressor with no heat transfer or pressure drop in the suction path, isobaric conditions during the admission and discharge processes with no backflow, absence of leakage in the compression chamber, no-slip condition in the electric motor, and no clearance volume. The theoretical mass flow rate of can be calculated from the following equation:

$$\dot{m}_{th} = \frac{N\, \rho_{sl} \forall_{sw}}{60}, \tag{6}$$

where N represents the nominal rotational speed of the compressor, ρ_{sl} in the gas density at the suction line, and $\forall_{sw}$ is the total volume swept by the piston.

Thus, the volumetric efficiency can be written as

$$\eta_v = \frac{\dot{m}}{\dot{m}_{th}} = \frac{\dot{m}_{th} - \Delta\dot{m}_{total}}{\dot{m}_{th}}, \tag{7}$$

where the actual mass flow rate can be written as the theoretical mass flow rate minus the total mass flow reduction, $\Delta\dot{m}_{total}$, brought about by different inefficiencies (Santos and Deschamps, 2020; Silva et al., 2022).

3.2 Exergy loss

The second law of thermodynamics allows estimates of energy inefficiencies based on the destruction of exergy (irreversibility or entropy generation). The exergy of a system corresponds to the maximum useful work that can be obtained by allowing the system to come into equilibrium with the dead state. The second law establishes that exergy is preserved in reversible processes and destroyed in real processes. Like energy, exergy can be transferred between systems through interactions in the form of heat, work, and mass transport. Therefore, the exergetic efficiency (η_{exe}) of a system is defined as the ratio between the minimum required power (reversible power, $\dot{W}$rev) and the actual power supplied ($\dot{W}$ele) to change the thermodynamic state of a fluid, that is:

$$\eta_{exe} = \frac{\dot{W}_{rev}}{\dot{W}_{ele}}, \tag{8}$$

The exergetic efficiency can also be written as a function of the total exergy loss ($\dot{\mathrm{I}}_{\mathrm{d}}$), which can be fractionated into various irreversibilities associated with different processes during a compression cycle. Therefore, the exergetic efficiency of a compressor can be obtained by summing up the inefficiencies arising from different entropy generation mechanisms, as follows:

$$\eta_{exe} = \frac{\dot{W} - \dot{\mathrm{I}}_d}{\dot{W}}, \tag{9}$$

Thus, the power supplied to the compressor can be broken down into the reversible power required to perform the different thermodynamic processes and the power consumed by irreversibility that reduce the exergetic efficiency of the compressor. These irreversibilities can be fractionated among the various components of the compressor. All exergy loss rates (irreversibility) can be calculated from the entropy generation, $\dot{S}ger$, and the dead state temperature, $Tamb$, using the Gouy-Stodola relationship (Eq. 10). Details the method to estimate all irreversibilities of reciprocating compressors are available in Araujo and Deschamps (2020).

$$\dot{I} = T_{amb}\dot{S_{ger}}, \tag{20}$$

4. RESULTS

The main objective of this article is to analyze the compressor performance associated with suction valves located on the cylinder head and on the piston, considering the same boundary conditions and compressor speed range. The dynamic characteristics of the valves and the suction orifice area were the same for both configurations. Exergy loss, valve impact speed, valve displacement, and volumetric inefficiencies were adopted to assess the differences between the different compressor designs. The simulations of both designs adopted an ideal discharge valve to avoid any effect of its dynamics on the suction valves.

4.1 Valve displacement

Figure 3 presents a comparison between the displacements of the suction valves on the cylinder head and on the piston head. As can be seen, the valves open four times throughout the suction process when the compressor operates under 2800 rpm, and three times under 6300 rpm, regardless of where the valve is installed. As shown in Figure 3a, the displacements of both valves are virtually the same, corroborating the findings of Wu et al. (2022). Due to the auxiliary force provided by the piston motion for the valve, the first opening reaches the maximum lift. However, the subsequent openings occur when the piston is decelerating and this acts to restrict the valve opening. This explains why the valve on the piston reaches smaller displacement on the third and fourth openings in comparison with valve on the cylinder head. Despite these differences, both valves close at the same time.

When the compressor operates under 6300 rpm (Figure 3b), the effects of the piston motion become more noticeable. Figure 3b shows that the displacement of first opening of valve on the piston is slightly greater than that of the valve on the cylinder head. However, the force resulting from the piston motion significantly reduce the valve displacements and the valve on the piston close earlier than the valve in the cylinder head, also reducing backflow.

The differences between displacements of both valves can also be seen in terms of root-mean-square error (RMSE) shown in Figure 6. This parameter is a commonly used metric to evaluate the similarity between curves. By calculating the average squared differences between the reference values (displacement of the suction valve on the cylinder head) and observed values (displacement of the suction valve on the piston), RMSE provides a quantitative measure of the overall difference between the two curves. As expected, the RMSE is almost negligible at low speeds and increases with the compressor speed. These results show that the effects of the piston motion at the valve cannot be neglected when the compressor operates under high speed.

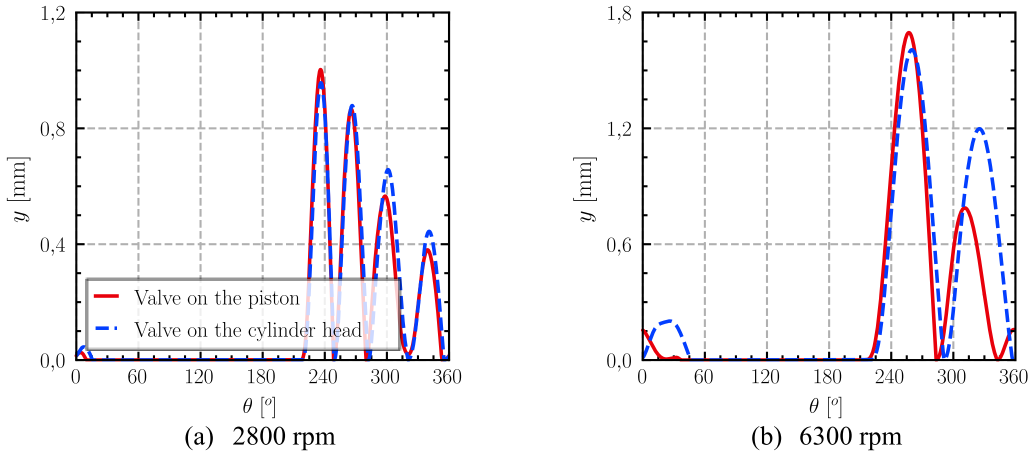

Figure 5 - Displacement of the valves on the cylinder head and on the piston for two different rotational speeds.

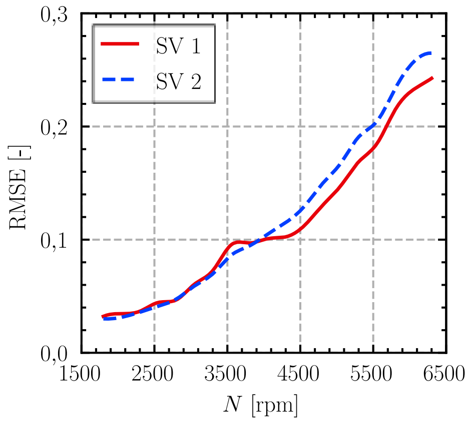

Figure 6 - Root mean square error between the valves on the cylinder head and on the piston.

4.2 Valve impact velocity

The valve impact velocity is an important parameter of valve design, being crucial to guarantee its value do not exceed the limit established for valve reliability. Figure 7 shows the impact velocity for the two suction valves (suction valve 1 and suction valve 2) adopted in both configurations. The results indicate that the impact velocity is greater for the valve on the piston, particularly under compressor high speeds, which is a consequence of the greater displacements observed in the first valve oscillation (Figure 5).

A significant difference is observed between the impact velocities predicted for valve 1 and valve 2 on the cylinder head. On the other hand, only a small difference is noticeable for the valves on the piston configuration, which suggests that the piston motion have a greater effect on the impact velocity than on the valve dynamics. This is in disagreement with Wu et al. (2022) who observed that the impact velocity is reduced when the valve is placed on the piston. Despite this disagreement, as in the present analysis Wu et al. (2022) suggest to increase the reed stiffness to reduce valve displacements in the first opening.

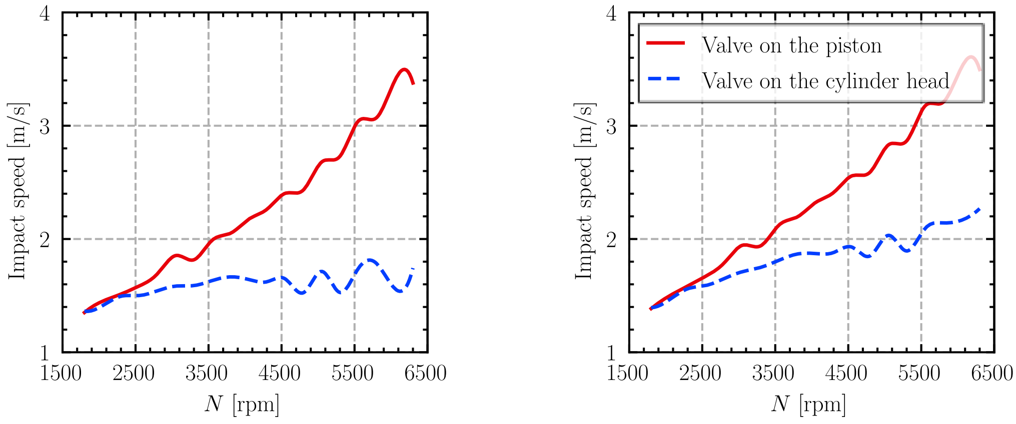

(a) Suction valve 1 (b) Suction valve 2

Figure 7 - Comparison between the impact speed for valve on the cylinder head and valve on the piston

4.3 Volumetric efficiency

Figure 8 shows the volumetric inefficiencies related to the suction gas path. As depicted in Figure 8a, the suction valve on the piston configuration has negligible backflow due to its earlier closure compared to the suction valve on the cylinder head. In contrast, Figure 8b shows that the suction valve on the piston has higher inefficiencies than the suction valve on the cylinder head when the compressor operates under speeds higher than 3300 rpm. This can be attributed to the piston inertial effects, which reduce the mass flow rate. At lower rotational speeds, the volumetric inefficiency of the valve on the cylinder head is greater due to the higher displacement of the first opening, acting to reduce the head loss.

As far as supercharging is concerned (Figure 8c), no significant differences are observed up to around 3300 rpm. Under higher speeds an offset is clearly seen between the results. It is interesting to notice that although the valve on the piston closes faster than the valve on the cylinder head, the supercharging effect is still present since the valve closes after the bottom dead center. This can be observed especially for speeds higher than 5800 rpm, where the supercharging effects are even greater for the valve on the piston configuration.

Figure 8d presents the inefficiencies due to heat transfer between the gas and the hot walls in the suction muffler. The piston configuration is prone to higher inefficiency due to its contact with the piston walls, which have higher temperature in comparison with the temperature of suction muffler walls. The results also show that this inefficiency does not vary significantly with the compressor speed.

The overall volumetric efficiency that results for the valve on the piston is consistently lower than that of for the valve on the cylinder head (Figure 9), as a consequence the higher inefficiencies discussed with the assistance of Figure 8. The difference between the two configurations is 3% under 1800 rpm, but it is greater than 5% at 6300 rpm. This is primarily due to the inefficiencies in the suction process (Figure 8b), being affected by valve fluttering which can vary with the rotational speed.

4.4 Exergy loss

Despite the considerable impact that the suction process has on the volumetric efficiency (as illustrated in Figure 8b), the configuration of the suction valve does not result in a significant difference in the specific exergy loss (exergy loss divided by the compressor mass flow rate) as indicated in Figure 10a. The valve on the piston even results in higher exergetic efficiency for rotational speeds below 3500 rpm, probably because the volumetric loss during the suction process reduces mass flow rate and hence viscous friction. However, beyond this threshold, the specific exergy loss reaches a peak of 6.28 kJ/kg for the valve on the piston and 6.04 kJ/kg for the valve on the cylinder head, a difference of 4%.. Because the mass flow rate is greater for the valve located on the cylinder head.

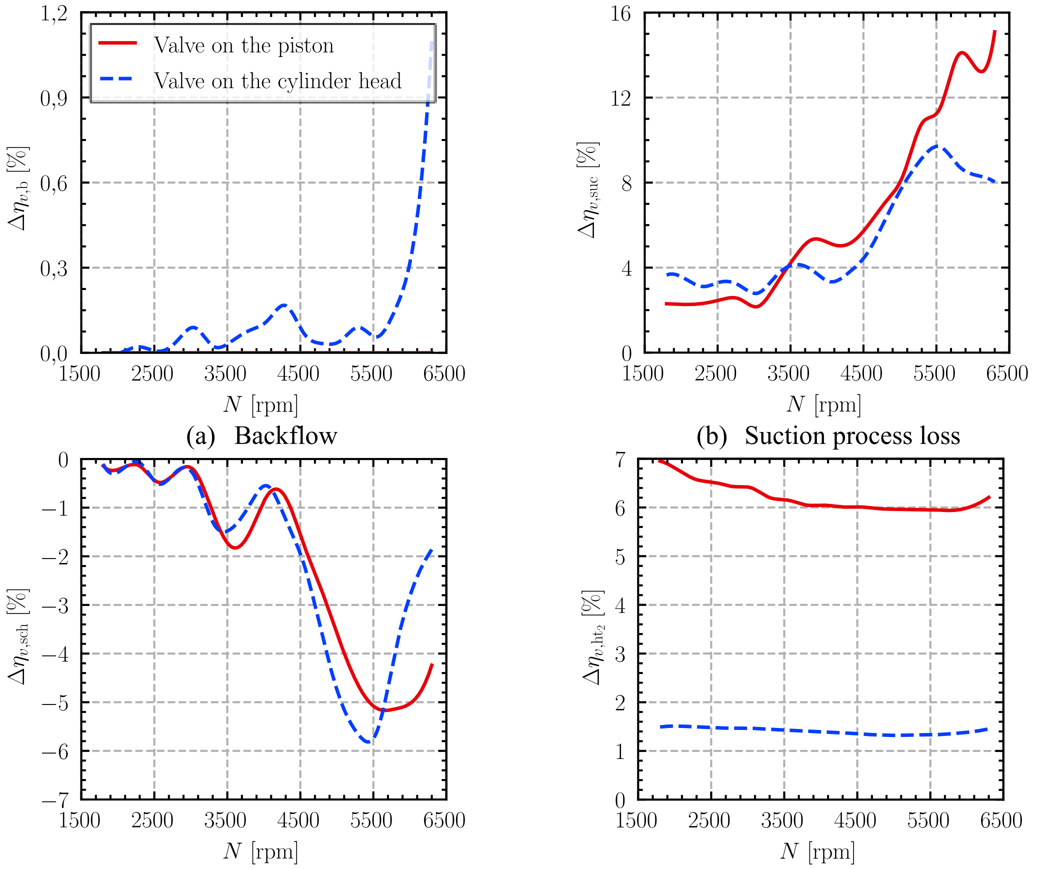

(a) Backflow (b) Suction process loss

(c) Supercharging (d) Heat transfer in suction muffler walls

Figure 8 - Volumetric inefficiencies associated with the valves on the cylinder head and on the piston.

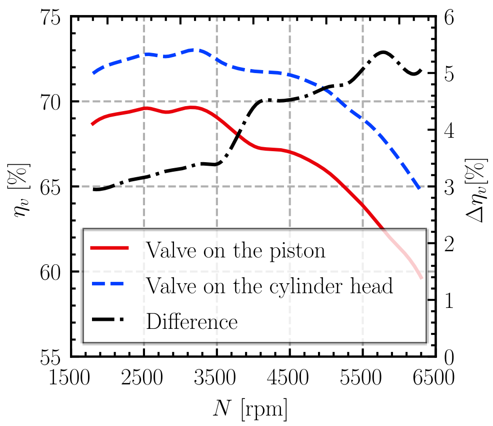

Figure 9 - Overall volumetric efficiency for the compressor with suction valves on the piston and on the cylinder head

Regarding the heat transfer irreversibility, Figure 10b shows quite different results for both configurations. Since the inlet temperature of the refrigerant is equal in both cases, greater entropy is produced during the suction process with the valve on the piston, mainly due to the greater temperature difference between the refrigerant the walls. This irreversibility is seen to decrease with the compressor speed regardless the valve configuration because the heat transfer coefficients also increase with the speed, resulting in reduced temperature differences, and hence lower entropy generation. The most substantial difference between the two valve configurations is evident for the compressor operating under 1800 rpm, in which case the irreversibility observed for the valve on the piston is 17.5% higher than that for the valve on the cylinder head.

Figure 11 presents the comparison between the exergetic efficiencies for both valve configurations. It is important to mention these exergy efficiencies are overestimated because an ideal discharge valve was adopted in the simulations. As indicated, the exergetic efficiency is consistently higher for the valve on the cylinder head throughout the entire operating speed range, primarily due to the smaller heat transfer irreversibility. The difference in efficiency is almost constant, reaching a maximum of 1.9% at 1800 rpm and a minimum of 1.5% at 3300 rpm. The average difference between the efficiencies is 1.7%.

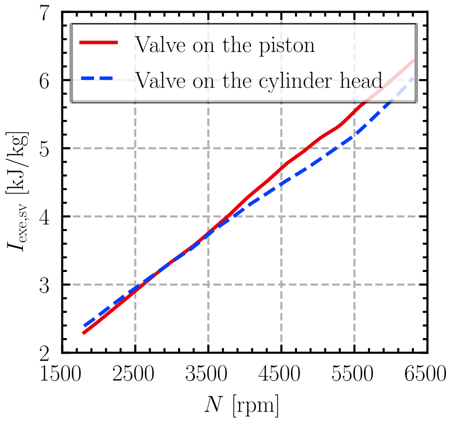

(a) Suction valves

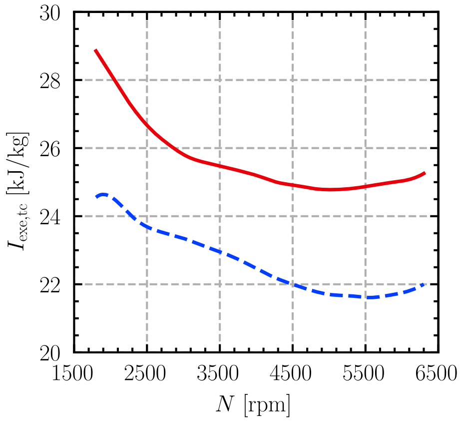

(b) Heat transfer

Figure 10 - Specific exergy losses at the suction valves (a) and due to heat transfer (b) for both valve configurations.

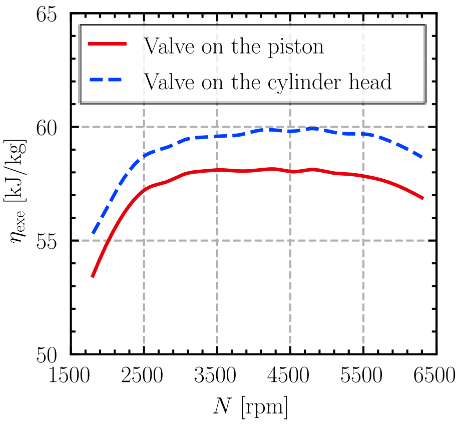

Figure 11 - Exergetic efficiency for both valve configurations.

5. CONCLUSIONS

The main objective of this study was to compare the behavior of compressors with suction valves positioned on the cylinder head and on the piston. The findings revealed that there was almost no difference in the displacements of the valves in both configurations at low speeds, corroborating previous findings. However, at higher speeds, the valve on the piston displayed a greater displacement and opened slightly earlier compared to the valve on the cylinder head. Nevertheless, during subsequent valve oscillations, the valve on the piston exhibited lower displacement compared to the valve on the cylinder head. The study also examined the volumetric inefficiencies associated with the suction process. It was observed that the piston configuration gives rise to higher inefficiencies due to the inertial effects of the piston. The volumetric efficiency of the valve on the piston configuration was found to be consistently lower than that of the valve on the cylinder head due to greater losses during the suction process. Overall, the results suggest that the configurations tested for the suction valve does not significantly affect the exergy loss. However, heat transfer irreversibility should be considered when choosing the valve configuration, since it can significantly affect the exergetic efficiency. These findings provide valuable insights into the compressor performance with different suction valve setups, which is useful for design optimization.

6. ACKNOWLEDGEMENTS

The authors appreciate the support from Nidec-GA and EMBRAPII (“Development of new technologies for refrigeration compressors” Project). Additional funding was provided by the National Institutes of Science and Technology (INCT) Program (CNPq Grant No. 404023/2019-3; FAPESC Grant No. 2019TR0846).

7. REFERENCES

Araujo, I. M.; Deschamps, C. Exergy Analysis Of Hermetic Reciprocating Compressors Adopted In Household Refrigeration Systems. In: Proceedings Of The 18th Brazilian Congress Of Thermal Sciences And Engineering. Abcm, 2020. Available In: <http://abcm.org.br/anais-de-eventos/cit20/0326>.

Deschamps, C. J.; Possamai, F. C.; Pereira, E. L. L. Numerical Simulation Of Pulsating Flow In Suction Mufflers. In: International Compressor Engineering Conference., 2002. Available In: <Https://Docs.Lib.Purdue.Edu/Icec>.

Disconzi, F. P.; Deschamps, C. J.; Pereira, E. L. Development Of An In-Cylinder Heat Transfer Correlation For Reciprocating Compressors. In: Proc. Int. Compressor Engineering Conference At Purdue., 2012. Available In: <https://docs.lib.purdue.edu/icec/2103/>.

Lemmon, E. W.; Bell, I. H.; Huber, M. L.; Mclinden, M. O. Nist Standard Reference Database 23: Reference Fluid Thermodynamic And Transport Properties-Refprop, Version 10.0, National Institute Of Standards And Technology. Standard Reference Data Program, Gaithersburg, 2018.

Link, R.; Deschamps, C. J. Numerical Analysis Of Transient Effects On Effective Flow And Force Areas Of Compressor Valves. In: International Compressor Engineering Conference., 2010. Available In: <https://docs.lib.purdue.edu/icec/1996>.

Pereira, E. L.; Deschamps, C. J. Influence Of Piston On Effective Areas Of Reed-Type Valves Of Small Reciprocating Compressors. Hvac And R Research, V. 17, P. 218–230, 4 2011. Issn 10789669.

Pizarro-Recabarren, R. A.; Barbosa, J. R.; Deschamps, C. J. Modeling The Stiction Effect In Automatic Compressor Valves. International Journal Of Refrigeration, V. 36, P. 1916–1924, 11 2013. Issn 01407007.

Santos, L. M.; Deschamps, C. J. Characterization Of Volumetric Inefficiencies Of Reciprocating Compressors Adopted In Small Capacity Refrigeration Systems. In: Proceedings Of The 18th Brazilian Congress Of Thermal Sciences And Engineering - Encit 2020, 2020.

Silva, W. T. F. D. da; Yupa-Villanueva, R.; Deschamps, C. J. Numerical Analysis Of Volumetric Inefficiencies Of A Small Variable Capacity Reciprocating Compressor. In: Proceedings Of The 19th Brazilian Congress Of Thermal Sciences And Engineering - Encit 2022., 2022.

Wu, W.; Guo, T.; Peng, C.; Li, X.; Li, X.; Zhang, Z.; Xu, L.; He, Z. Fsi Simulation Of The Suction Valve On The Piston For Reciprocating Compressors. International Journal Of Refrigeration, V. 137, P. 14–21, 2022. Issn 0140-7007. Available in: <https://www.sciencedirect.com/science/article/pii/s0140700722000305>.

8. RESPONSIBILITY NOTICE

The authors are the only responsible for the printed material included in this paper.